ENERGY AND EXERGY ANALYSIS OF A HYBRID ORC POWER PLANT

Nedžad R. RUDONJA*, **Nada S. MILUTINOVIĆ**, **Miloš J. BANJAC**, **Ivan J. ZLATANOVIĆ**, **Ružica I. TODOROVIĆ**

University of Belgrade, Faculty of Mechanical Engineering, Kraljice Marije 16, 11120 Belgrade, Serbia

*Corresponding author: nrudonja@mas.bg.ac.rs

Organic Rankine cycles (ORCs) are highly recommended technology to generate electricity from low-temperature sources such as geothermal sources. The performance of the cycle mostly depends on operation conditions, installed equipments and selection of working fluid. This paper presents a comparative energy and exergy analysis of a geothermal-biomass Organic Rankine cycle (ORC) for three working fluids: R113, R245fa, and R600a. In addition, analyzed ORC is compared with the Rankine cycle that runs on Serbian lignite from the aspect of equivalent CO_2 *emission and necessary primary energy. The analyzed system is an ORC power plant with two heat sources – geothermal water from Vranjska Banja and wood biomass. The results revealed the highest thermal and exergy efficiency with R113, 14.53%, and 41.64%, respectively, as well as the turbine power output of 4.21 MW with 73.20 kW pump power input. Exergy analysis showed the highest exergy destruction rate in the heat exchanger with flue gases made by wood combustion (80-89%) and the highest obtained exergy efficiency of 41.64% in the case of R113. If the power plant used Serbian lignite as a fuel for the same thermal power input, it would need between 133-169 kt/year of lignite, which would result in* CO_2 *emission of around 63-80 kt/year.*

Keywords: ORC, working fluid selection, biomass, geothermal energy

1. Introduction

One of the biggest challenges that current and future generations must overcome is finding adequate renewable energy technologies capable of meeting the rapidly increasing global energy demand while replacing conventional fossil fuel technologies [1]. Low-temperature heat sources, such as geothermal energy, have garnered significant research interest [2]. Geothermal power plants are independent of weather conditions, enabling them to supply baseload electricity an essential advantage over other renewable technologies like solar or wind energy.

Geothermal source temperatures can reach up to 350 °C, with the technological lower limit for power generation around 80 °C [3]. In 2020, 14,050 MW of geothermal capacity was installed worldwide, with most installations located in the USA, Indonesia, the Philippines, and Turkey (fig. 1).

Different thermodynamic cycles can be utilized with geothermal sources depending on their temperature. Examples include the Steam Rankine Cycle (SRC), Organic Rankine Cycle (ORC) and Kalina Cycle. It is well known that SRC requires higher operating parameters to achieve satisfactory cycle efficiencies.

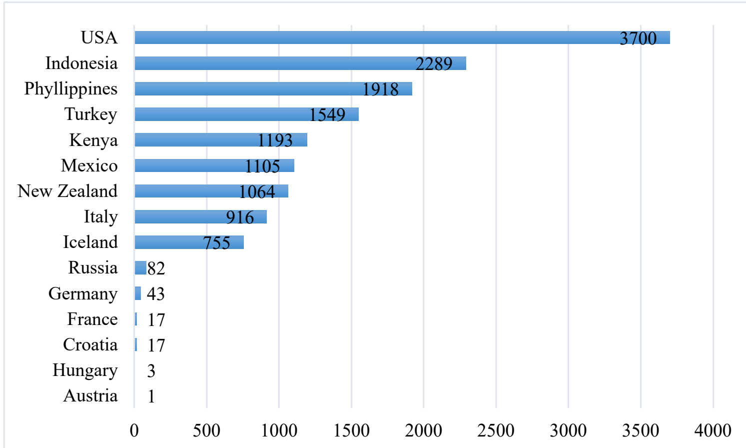

Figure 1: The installed capacity in geothermal power plants for electricity production, worldwide, (MWel), 2020 (Huttrer, 2020)

Considering that only a small portion of geothermal sources have temperatures above 100 °C, SRC is not a very common choice. ORC, which uses organic fluids as working fluids, is highly recommended for low-temperature heat sources [3]. It is primarily used with geothermal [4] and solar sources [5], but waste heat recovery [6] and biomass combustion [7] are also gaining popularity, along with hybrid concepts such as geothermal-solar systems [8].

Research on ORCs can be divided into three main areas: possible configurations [9], working fluid selection [10], and optimization of cycle parameters [11]. Basaran et al. [12] investigated the effect of different refrigerants on the performance of binary geothermal power plants from the perspective of the First and Second Laws of Thermodynamics. Their analysis showed that dry refrigerants, such as R600 and R600a, exhibit higher thermal and exergy efficiencies than wet refrigerants like R134a and R152a.

In the study by Kankeyan et al. [13], the thermal efficiencies of 72 working fluids in a simple ORC were investigated. The results were presented in terms of preferred working fluids for different temperature ranges. For instance, MD_2M and cyclopentane are recommended for temperatures between 50–100 °C; butane, neopentane, and R245fa for 100–150 °C; ethanol, methanol, and propanone for 150–200 °C; and water, m-xylene, and p-xylene for 200–320 °C.

Herath et al. [14] emphasized that many previously established selection criteria for refrigerants are no longer applicable due to the phase-out of chlorofluorocarbons (CFCs), the ongoing phase-down of hydrochlorofluorocarbons (HCFCs), and restrictions on substances with high ozone depletion potential (ODP) and global warming potential (GWP). Therefore, the authors examined the performance characteristics of ORCs in relation to pressure and evaporating temperature using R134a, R245fa, benzene, methanol, ethanol, acetone, and propane. They concluded that the thermal efficiency of the ORC increases with higher evaporator temperature and pressure, while decreasing condenser operating temperature and pressure has the same effect.

This paper presents a simulation study of a power plant utilizing renewable energy sources available in southern Serbia, specifically geothermal energy from Vranjska Banja and wood biomass, in a simple ORC. The analysis was conducted from the perspective of the First and Second Laws of Thermodynamics.

Additionally, thermodynamic results were compared for three different working fluids: R113, R245fa, and R600a.

Furthermore, based on the Rulebook on Energy Efficiency [15], the approximate amount of primary energy required annually to achieve the same thermal power output was calculated, along with the corresponding CO_2 emissions if Serbian lignite were used instead of the aforementioned renewable sources. To the best of the author's knowledge, this type of study has not been previously conducted for this geographical area, despite Serbia's significant geothermal potential [16][17], which could contribute to achieving net-zero emissions.

2. Main characteristics of the exploration area

According to the Energy Development Strategy of the Republic of Serbia to 2025 with Projections to 2030 (Ministry of Mining and Energy, 2016), the total potential of renewable energy sources is 5.65 Mtoe per year, while the geothermal potential is estimated at 0.18 Mtoe per year [18]. The Statistical Office of the Republic of Serbia reports that only 0.01% of geothermal energy in primary energy production has been utilized for electricity generation, as shown in fig. 2.

The warmest thermal springs in Serbia include Vranjska Banja, Jošanička Banja, Sijarinska Banja, Kuršumlijska Banja, and Novopazarska Banja, all with temperatures exceeding 50 °C [19].

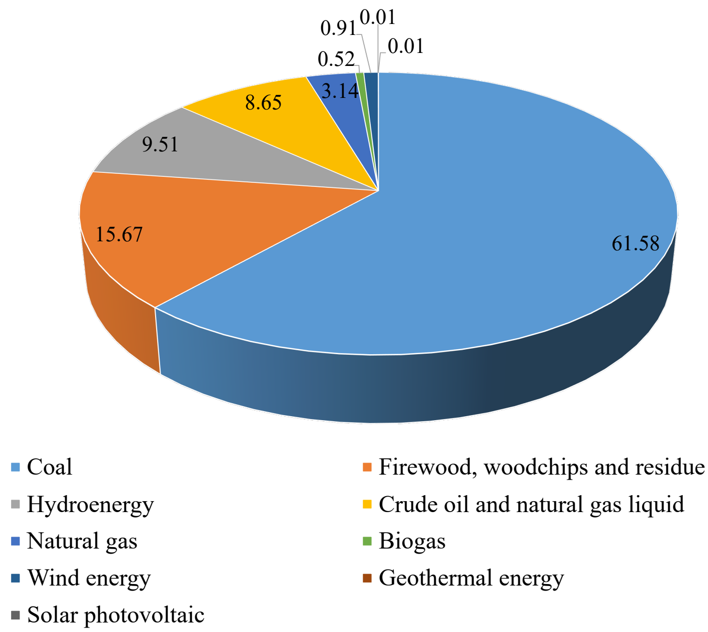

Figure 2: Primary energy production, Serbia, (%), 2021) [20]

The City Municipality of Vranjska Banja is located in southeastern Serbia. Most of the springs in Vranjska Banja are capped by a collecting channel, and these are the ones considered in this paper. Table 1 provides an overview of the wells in Vranjska Banja.

Geothermal water emerges within a thermal spring zone with active surface sources spanning an area of 500 × 200 m [16]. The thermal water from these springs is artesian, meaning it rises naturally to the Earth's surface due to internal overpressure. As a result, no additional energy is required for its extraction.

Table 1: Main features of springs in Vranjska Banja [21]

	Name	Discharge of springs [kg/s]	Depth [m]	Temperature [°C]
1	Upper Spring	1.2	-	78
2	Spring B-1	2	26	92
3	Spring A-1	0.5	2	91
4	VG-2	27	163	111
5	Spring A-3	2.1	20	91
6	Spring B-2	1	7	96
7	Spring B-3	1.5	12	87
8	Spring A-2	1	25	84
9	VG-3	21.5	160	120
10	Collecting channel	50-70	-	84

3. Organic rankine cycle

The schematic of the analyzed ORC system is shown in fig. 3. The configuration investigated in this study is a simple ORC, consisting of a turbine and generator mounted on the same shaft, a condenser, a pump, and two heat exchangers for two different heat sources.

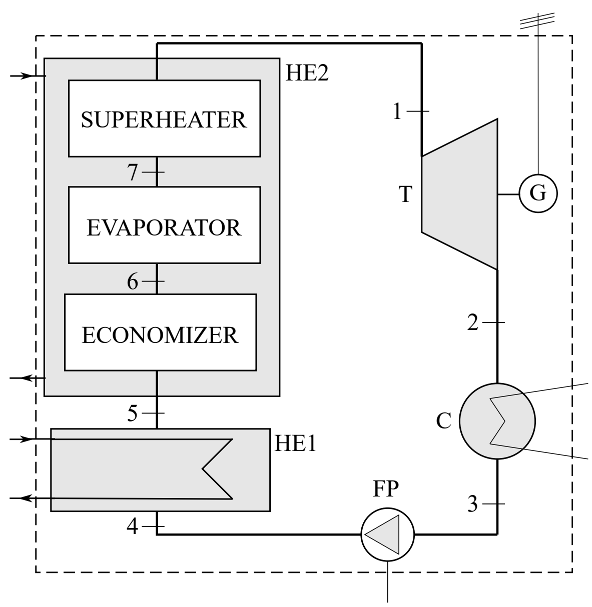

Figure 3: Schematic of the ORC system: turbine (T), generator (G), condenser (C), feed pump (FP), heat exchanger with geothermal water (HE 1), and heat exchanger with flue gases from wood combustion (HE 2)

The flow process through the components is shown in fig. 4. The high-pressure vapor organic fluid is directed through the turbine, where its thermal energy is converted into mechanical energy of the shaft as it expands to a lower pressure. The mechanical energy produced in the turbine is then converted into electrical energy by the generator connected to the turbine. In the condenser, the low-pressure vapor is condensed into a saturated liquid using cooling water and subsequently pressurized by the pump. In the heat exchangers, the working fluid is vaporized and superheated before entering the turbine.

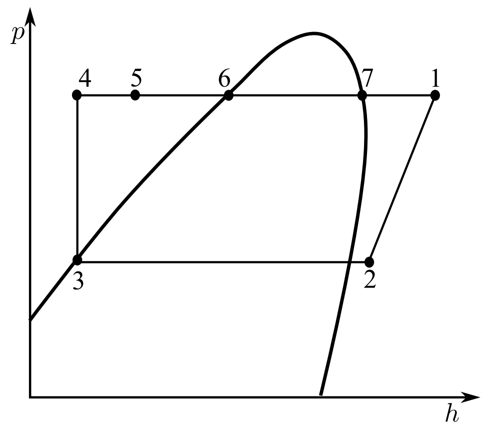

Figure 4: $p - h$ (pressure–specific enthalpy) diagram of the analyzed ORC

4. Working fluid selection

The selection of working fluid is crucial when analyzing the ORC system, as it is directly linked to cycle efficiency, net power output, the size of heat exchangers and turbines, as well as capital and maintenance costs [22]. Organic fluids operate at lower pressures and have a lower evaporating temperature, which allows them to utilize low-temperature heat sources. Additionally, the entropy difference between the saturated liquid and saturated vapor of organic fluids is significantly smaller compared to water, resulting in lower latent heat, as shown in fig. 5.

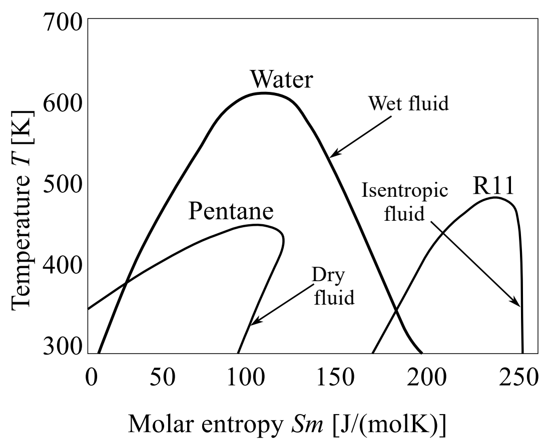

Figure 5: Types of working fluids: wet fluid, dry fluid, and isentropic fluid.

Table 2: Properties of working fluids: R113, R245fa, and R600a [23]

Properties	**R113**	**R245fa**	**R600a**
Chemical formula	$C_2Cl_3\ F_3$	$C_3\ F_5H_3$	C_4H_{10}
Class	CFC	HFC	HC
Type	Dry	Dry	Dry
Boiling temperature ($^\circ$C)	47.7	14.90	-11.67
Critical temperature ($^\circ$C)	214.06	154.05	134.67
Critical pressure (bar)	33.92	36.4	36.4

Table 3: Set parameters for the simulation of the ORC system

Evaporating	$T_e = T_6 = (120 + 273.15)\mathrm{K}$ $p_e = p_6 = p_{\text{sat}}\ (T_e)$	
Condensing	$T_c = T_2 = (35 + 273.15)\mathrm{K}$ $p_c = p_{sat}\,(T_c)$	
Component	Parameters	
Turbine $\eta_{iT} = 0.85$	Inlet	$T_1 = (130 + 273.15)\mathrm{K}$ $p_1 = p_e$
	Outlet	$p_2 = p_c$
Condenser	Inlet	$T_2 = (35 + 273.15)\mathrm{K}$ $p_2 = p_c$
	Outlet	$p_3 = p_c$
Pump $\eta_{iP} = 0.75$	Inlet	$p_3 = p_c$ $h_3 = h_{\text{sat}}\ (p_c)$
	Outlet	$p_4 = p_e$
Heat Exchanger 1	Inlet	$T_{\text{gw,out}} = (60 + 273.15)\mathrm{K}$ $\dot{m}_{\text{gw}} = 50\ \mathrm{kg/s}$
	Outlet	$T_{gw,in} = (84 + 273.15)\mathrm{K}$ $T_5 = T_{gw,in} - 10\ \mathrm{K}$
Heat Exchanger 2	Inlet	$p_5 = p_e$ $T_5 = T_{gw,in} - 10\ \mathrm{K}$
	Outlet	$T_1 = (130 + 273.15)\mathrm{K}$ $p_1 = p_{\mathrm{e}}$

5. Thermodynamic model

There are various methodologies to assess the performance of a cycle, with energy and exergy analysis being among the most commonly used. To establish a thermodynamic model of the cycle, the following assumptions are made:

1. The ORC is considered a stable cycle with no leakage of the working fluid;
2. Pressure drops and heat transfer losses in the system are neglected;
3. The pump and turbine operate adiabatically with specified isentropic efficiencies; and
4. At the condenser outlet, the working fluid is in the saturated liquid phase.

The numerical assumptions regarding modeling the ORC system are given in tab. 3.

5.1. Energy analysis

The mass flow rate of the working fluid in ORC is determined from HE 1 using eq. (1):

$$\dot{Q}_{\text{gw}} = \dot{m}_{\text{gw}} c_{p,\text{gw}} \left(T_{\text{gw,in}} - T_{\text{gw, out}}\right) = \dot{m}_{\text{f}} \left(h_6 - h_5\right) \tag{1}$$

where $\dot{Q}_{\text{gw}}$ is the heat transfer rate of HE 1 (kW), $\dot{m}_{\text{gw}}$ is the mass flow rate of geothermal water (kgs^{-1}), $T_{\text{gw,in/out}}$ is inlet/outlet temperature of geothermal water (K), $c_{p,\text{gw}}$ is the specific heat capacity of geothermal water at a constant pressure $(\mathrm{kJkg}^{-1}\mathrm{K}^{-1})$, $\dot{m}_{\text{f}}$ is the mass flow rate of the working fluid (kgs^{-1}) and h_{i} (i=1..6) is specific enthalpy of working fluid in certain state point of cycle (kJkg^{-1}). The turbine power output is calculated using eq. (2):

$$P_{\text{T}} = \dot{m}_{\text{f}} \left(h_1 - h_2\right) \tag{2}$$

A certain amount of energy is required for the pump to pressurize the fluid, which is considered as power input. The power input is calculated using eq. (3):

$$P_{\mathrm{P}} = \dot{m}_{\mathrm{f}} \left(h_4 - h_3 \right) \tag{3}$$

Since the river Banjstica is located near the geothermal source, the adopted cooling system uses water from the river. The inlet parameters of the cooling water are set to 293.15 K and 304 kPa, while the outlet temperature is set to 353.15 K. The mass flow rate of the cooling fluid is determined using eq. (4):

$$\begin{aligned} \dot{Q}_{\mathrm{c}} &= \dot{m}_{\mathrm{f}} \left(h_2 - h_3 \right) = \dot{m}_{\mathrm{w}} \left(h_{\mathrm{w2}} - h_{\mathrm{w1}} \right) \\ \dot{m}_{\mathrm{w}} &= \frac{\dot{Q}_{\mathrm{c}}}{\left(h_{\mathrm{w2}} - h_{\mathrm{w1}} \right)} \end{aligned} \tag{4}$$

where $\dot{Q}_{\mathrm{c}}$ is the heat transfer rate in the condenser (kW), $h\mathrm{w}, i$ is the specific enthalpy of the cooling water at the inlet/outlet of the condenser (kJkg^{-1}), and $\dot{m}_{\mathrm{w}}$ is the mass flow rate of the cooling water (kgs^{-1}).

The thermal efficiency of the ORC cycle is determined in eq. (5):

$$\eta_{\mathrm{th}} = 1 - \frac{\left(h_2 - h_3 \right)}{\left(h_1 - h_4 \right)} \tag{5}$$

Wood is considered a significant source of renewable energy in Serbia, as forests cover approximately 27% of the country's territory. Various calculations related to the combustion process of wood biomass are conducted for HE 2, based on the assumed as-received composition of the biomass.

Boiler efficiency is the ratio of the useful output energy of a boiler to the input energy, and it is assumed to be $\eta_{\mathrm{b}} = 88\%$. The lower heating value (LHV) is calculated using eq. (6) [24] for the wood biomass shown in fig. 6.

$$LHV = 340 \cdot C + 1200 \cdot (H - O/8) + 105 \cdot S - 25 \cdot M \tag{6}$$

The mass flow rate of biomass fed to the boiler is calculated using eq. (7):

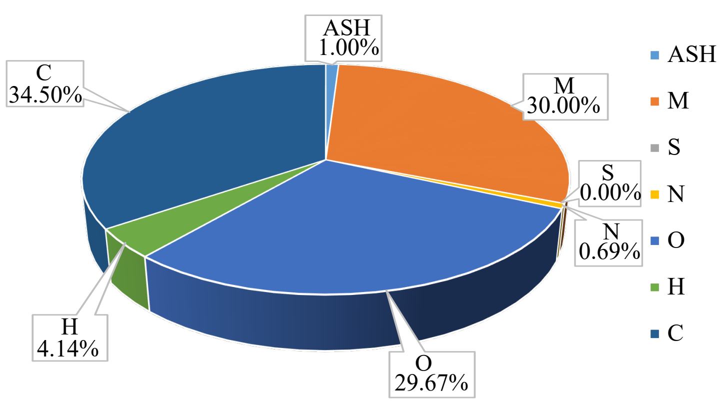

Figure 6: Ultimate analysis of wood biomass, where C, H, O, N, S, M, and ASH represent the weight percentages of carbon, hydrogen, oxygen, nitrogen, sulfur, moisture, and ash, respectively, in the as-received mass of wood (%)

$$\begin{aligned} \dot{Q}_{\mathrm{HE2}} &= \dot{m}_{\mathrm{f}} \left(h_1 - h_5 \right) = \dot{m}_{\mathrm{bm}} \eta_{\mathrm{b}} LHV \\ \dot{m}_{\mathrm{bm}} &= \frac{\dot{Q}_{\mathrm{HE2}}}{\eta_{\mathrm{b}} LHV} \end{aligned} \tag{7}$$

where $\dot{Q}_{\mathrm{HE2}}$ is thermal power rate of HE 2 (kW), $\dot{m}_{\text{bm}}$ is the mass flow rate of biomass (kgs^{-1}), and LHV is the lower heating value of wood biomass (kJkg^{-1}).

5.2. Exergy analysis

Exergy analysis is performed for the components of the ORC system, where: h_0 is the specific enthalpy of the working fluid, s_0 is the specific entropy of the working fluid, h_{w0} is the specific enthalpy, and s_{w0} is the specific entropy of the cooling water at the ambient state, determined by the temperature of $T_0 = 20°\mathrm{C}$ and the pressure of $p_0 = 101.325\ \mathrm{kPa}$. eqs. (8–12) present the exergy analysis.

Turbine:

$$\begin{aligned}
\dot{E}_{x1} &= \dot{m}_{\mathrm{f}}\left(\left(h_1 - h_0\right) - T_o\left(s_1 - s_0\right)\right)\\
\dot{E}_{x2} &= \dot{m}_{\mathrm{f}}\left(\left(h_2 - h_0\right) - T_o\left(s_2 - s_0\right)\right)\\
\dot{E}_{x,\mathrm{T}} &= \left|P_{\mathrm{T}}\right| = \dot{m}_{\mathrm{f}}\left(h_1 - h_2\right)\\
\dot{E}_{x\mathrm{D,T}} &= \dot{E}_{x1} - \left(\dot{E}_{x,\mathrm{T}} + \dot{E}_{x2}\right)
\end{aligned} \tag{8}$$

Condenser:

$$\begin{aligned}
\dot{E}_{x3} &= \dot{m}_{\mathrm{f}}\left(\left(h_3 - h_0\right) - T_0\left(s_3 - s_0\right)\right)\\
\dot{E}_{x,\mathrm{w1}} &= \dot{m}_{\mathrm{w}}\left(\left(h_{\mathrm{w1}} - h_{\mathrm{w}o}\right) - T_0\left(s_{\mathrm{w1}} - s_{\mathrm{w0}}\right)\right)\\
\dot{E}_{x,\mathrm{w2}} &= \dot{m}_{\mathrm{w}}\left(\left(h_{\mathrm{w2}} - h_{\mathrm{w0}}\right) - T_0\left(s_{\mathrm{w2}} - s_{\mathrm{w0}}\right)\right)\\
\dot{E}_{x\mathrm{D,C}} &= \left(\dot{E}_{x2} + \dot{E}_{x,\mathrm{w1}}\right) - \left(\dot{E}_{x3} + \dot{E}_{x,\mathrm{w2}}\right)
\end{aligned} \tag{9}$$

Pump:

$$\begin{aligned}
\dot{E}_{x4} &= \dot{m}_{\mathrm{f}}\left(\left(h_4 - h_0\right) - T_0\left(s_4 - s_0\right)\right)\\
\dot{E}_{x,\mathrm{P}} &= P_{\mathrm{P}} = \dot{m}_{\mathrm{f}}\left(h_4 - h_3\right)\\
\dot{E}_{x\mathrm{D,P}} &= \left(\dot{E}_{x3} + \dot{E}_{x,\mathrm{P}}\right) - \dot{E}_{x4}
\end{aligned} \tag{10}$$

Heat Exchanger 1:

$$\begin{aligned}
&\dot{E}_{x,Q_{\mathrm{gw}}} = \dot{Q}_{\mathrm{gw}} - T_0\Delta S_{\mathrm{gw}} = \dot{Q}_{\mathrm{gw}} - T_0\dot{m}_{\mathrm{gw}}c_{p,\mathrm{gw}}\ln\frac{T_{\mathrm{gw,in}}}{T_{\mathrm{gw,out}}} = \dot{Q}_{\mathrm{gw}}\left(1 - \frac{T_0}{T_{\mathrm{gw,in}} - T_{\mathrm{gw,out}}}\ln\frac{T_{\mathrm{gw,in}}}{T_{\mathrm{gw,out}}}\right)\\
&\dot{E}_{x5} = \dot{m}_{\mathrm{f}}\left(\left(h_5 - h_0\right) - T_0\left(s_5 - s_0\right)\right)\\
&\dot{E}_{x\mathrm{D,HE1}} = \left(\dot{E}_{x4} + \dot{E}_{x,Q_{\mathrm{gw}}}\right) - \dot{E}_{x5}
\end{aligned} \tag{11}$$

Heat Exchanger 2:

$$\begin{aligned}
&\dot{E}_{x,Q_{\mathrm{fg}}} = \dot{Q}_{\mathrm{fg}} - T_0\Delta S_{\mathrm{fg}} = \dot{Q}_{\mathrm{fg}} - T_0\dot{m}_{\mathrm{fg}}c_{p,\mathrm{fg}}\ln\frac{T_{\mathrm{e,out}}}{T_{\mathrm{sh,in}}} = \dot{Q}_{\mathrm{fg}}\left(1 - \frac{T_0}{T_{\mathrm{e,out}} - T_{\mathrm{sh,in}}}\ln\frac{T_{\mathrm{e,\,out}}}{T_{\mathrm{sh,in}}}\right)\\
&\dot{E}_{x\mathrm{D,HE2}} = \left(\dot{E}_{x5} + \dot{E}_{x,Q_{\mathrm{fg}}}\right) - \dot{E}_{x1}
\end{aligned} \tag{12}$$

where $\dot{E}_{x1..6}$ is exergy flow working fluid of ORC of specific state (kW), $\dot{E}_{x,\mathrm{T}}$ is exergy of power of the turbine (kW), $\dot{E}_{x\mathrm{D,T}}$ is exergy destruction rate in the turbine (kW), $\dot{E}_{x,\mathrm{w1/w2}}$ is inlet/outlet exergy flow of cooling water in the condenser (kW), $\dot{E}_{x\mathrm{D,C}}$ is exergy destruction rate in the condenser (kW), $\dot{E}_{x,\mathrm{P}}$ is exergy of power of pump (kW), $\dot{E}_{x\mathrm{D,P}}$ is exergy destruction rate in pump (kW), $\dot{E}_{x,Q_{\mathrm{gw}}}$ is exergy of the heat of geothermal water, $\dot{E}_{x\mathrm{D,HE1}}$ is exergy destruction rate in HE 1 (kW), $\dot{E}_{x,Q_{\mathrm{fg}}}$ is exergy of the heat of flue gases (kW), $T_{\mathrm{e,\,out}}$ is outlet temperature of the flue gases in economizer (K), $T_{\mathrm{sh,in}}$ is inlet temperature of flue gases in superheater (K) and $\dot{E}_{x\mathrm{D,HE2}}$ is exergy destruction rate in HE 2 (kW).

Exergy efficiency is calculated in eq. (13):

$$\begin{aligned}
\eta_{\mathrm{ex}} &= \frac{\sum \dot{E}_{x,\mathrm{in}} - \sum \dot{E}_{x\mathrm{D}}}{\sum \dot{E}_{x,\mathrm{in}}} = 1 - \frac{\sum \dot{E}_{x\mathrm{D}}}{\sum \dot{E}_{x,\mathrm{in}}} \\
\dot{E}_{x,\mathrm{D}} &= \dot{E}_{x\mathrm{D,T}} + \dot{E}_{x\mathrm{D,C}} + \dot{E}_{x\mathrm{D,P}} + \dot{E}_{x\mathrm{D,HE1}} + \dot{E}_{x\mathrm{D,HE1}} \\
\dot{E}_{x,\mathrm{in}} &= \dot{E}_{x,Q_{\mathrm{gw}}} + \dot{E}_{x,Q_{\mathrm{fg}}} + \dot{E}_{x,\mathrm{P}}
\end{aligned} \tag{13}$$

5.3. Equivalent lignite consumption and CO_2 emission

This analysis aims to quantify the savings in fossil fuel consumption and CO_2 emission for our power plant with geothermal water and wood biomass compared to the plant that runs on lignite. Lignite consumption and CO_2 emission are estimated using [15] in two scenarios for the ORC system that has $\tau = 8,500\ \mathrm{h}$ operating time. The first scenario is the one previously analyzed where geothermal energy and biomass are used as fuel. The second scenario uses Serbian lignite with $LHV_{\mathrm{lignite}} = 6,700\ \mathrm{kJkg^{-1}}$ to generate electricity for the same thermal power input as used in the first scenario.

Lignite consumption is calculated in eq. (14):

$$\dot{m}_{\mathrm{lignite}} = \left(\dot{Q}_{\mathrm{gw}} + \dot{Q}_{\mathrm{HE2}}\right) \cdot \tau \cdot k_{\mathrm{lignite}} / LHV_{\mathrm{lignite}} \tag{14}$$

where k_{lignite} is the coefficient of conversion to primary energy (lignite) $(\mathrm{kgkWh^{-1}})$ equal to $k_{\mathrm{lignite}} = 1.3$ and τ operating time of plant equal to $\tau = 8,500\ \mathrm{h}$.

Equivalent CO_2 emission is determined in eq. (15):

$$\dot{m}_{\mathrm{CO_2}} = \left(\dot{Q}_{\mathrm{gw}} + \dot{Q}_{\mathrm{HE2}}\right) \cdot \tau \cdot k_{\mathrm{CO_2}} / LHV_{\mathrm{lignite}} \tag{15}$$

where $k_{\mathrm{CO_2}}$ is the coefficient of equivalent CO_2 emission for lignite as a primary energy source equal $k_{\mathrm{CO_2}} = 0.33\ \mathrm{kgkWh^{-1}}$.

6. Model validation

The model is validated against literature data and found to be in good agreement. To the author's knowledge, there are no available experimental data for this specific ORC configuration and parameters, so a detailed literature survey has been conducted to determine whether the obtained results are in agreement with the literature.

Table 4: A comparison of thermal and exergy efficiencies of the ORCs reported in the literature

Related study	Working fluid	Evaporating temperature (K)	Condensing temperature (K)	Thermal efficiency (%)	Exergy efficiency (%)
[25]	Isopentane	403.15	303.15	14.6	-
[26]	NH_3	$351.45 - 423.15$	$313.15 - 303.15$	12.8	41%
[27]	R 290	-	-	8.47	47.6
[28]	n -Pentane	-	-	10.7	29.6
[29]	R 600 a	401.15	284.85	10.2	33.5
[30]	R 134 a	350.75	291.15	11.24	39.03
Present study	R 113 R245fa R600a	393.15	308.15	$13.31 - 14.53$	$35.91 - 41.64$

7. Results and discussion

Considering that the thermal properties of analyzed working fluids are different, the thermodynamic performance of the cycle under the same heat source conditions will be different. While using organic fluids in ORCs with low-temperature heat sources, high mass flow rates of working fluids are expected because of their small vaporization enthalpy. Since the mass flow rate of the working fluid is directly related to the diameters of pipes and hence the capital and maintenance costs, the best result belongs to R600a with 51.78 kg/s and it is significantly lower in comparison to other fluids. For instance, R113 needs 165.33% and R245fa 83.75% higher mass flow rate than R600a for the same thermal input in HE 1 (fig. 7 a)). A similar conclusion can be drawn from fig. 7 b) where it is presented the mass flow rate of cooling water in the condenser.

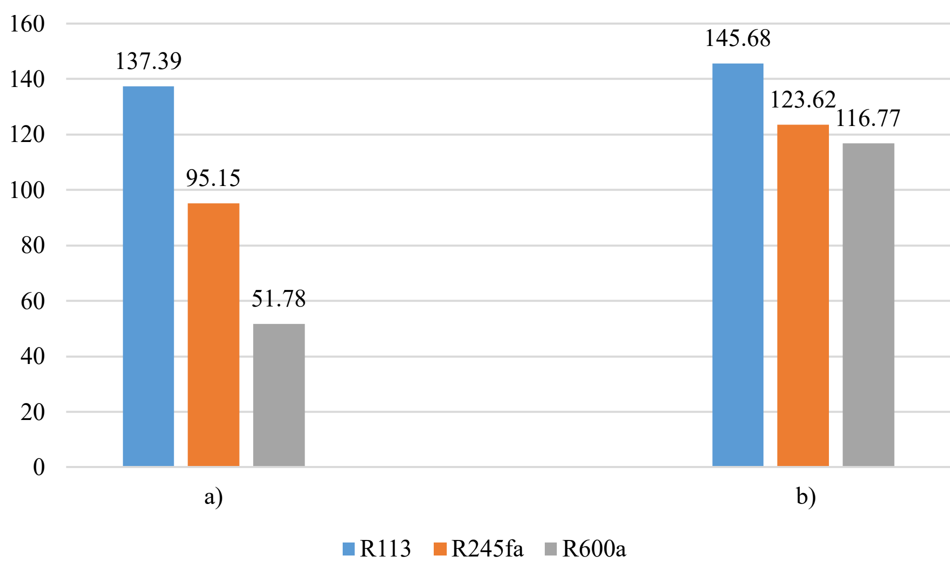

Figure 7: Mass flow rate (kg/s): a) working fluids in ORC, b) cooling water in the condenser

R113 provides 4.21 MW of turbine power output, which is the highest result amongst compared working fluids. In comparison to R113, R600a produces 21.6% less power output significantly decreasing generated electricity in the generator (fig. 8 a)). The pump consumption can be high for the ORCs and it is a result of the increased mass flow rate of the working fluid, which is necessary to be pressurized up to evaporation pressure. R600a needs 315.4% and R245fa 126.81% more power input than R113 (fig. 8 b)).

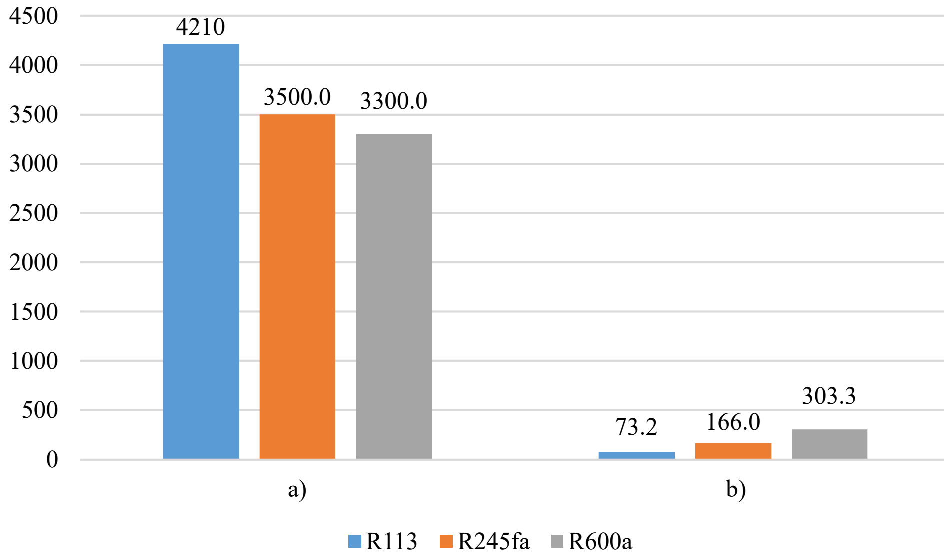

Figure 8: Power (kW): a) turbine, b) pump

As reported in tab. 4, thermal efficiencies of ORCs are usually lower than 15%. In our study, R113 obtained the highest thermal efficiency with 14.53%. There is a decrease in thermal efficiency of 8.3% for R600a compared to R113 which might be due to high pump consumption (fig. 9).

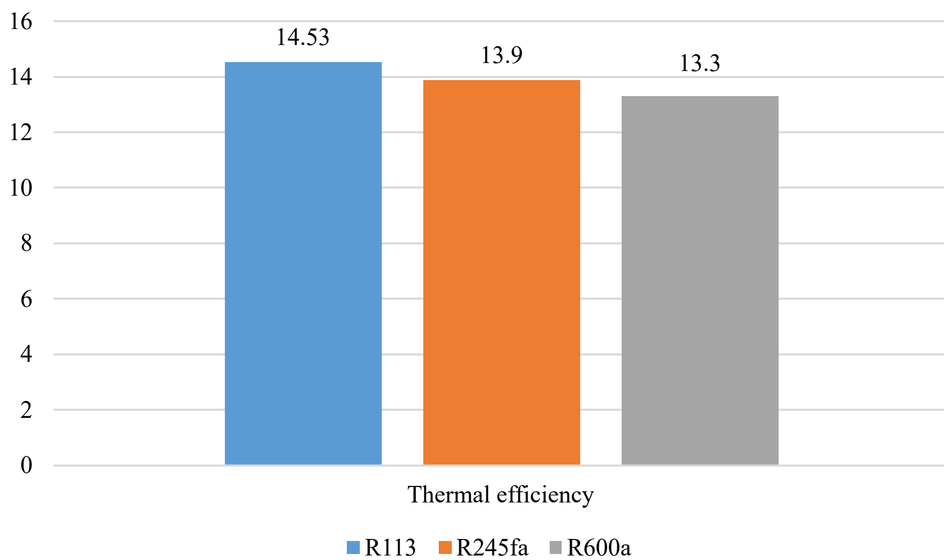

Figure 9: Thermal efficiency, (%)

According to [31], an analysis of the biomass combustion process was conducted, which gave results presented in tab. 5 and fig. 10.

Table 5: Temperatures of flue gases at the inlet/outlet of heat exchanger units of HE 2

Temperature (K)	Position	**R113**	**R245fa**	**R600a**
Super-heater	Inlet	1013.15	1013.15	1013.15
	Outlet	985.48	970.46	948.42
Evaporator	Inlet	985.48	970.46	948.42
	Outlet	568.00	628.60	682.51
Economizer	Inlet	568.00	628.60	682.51
	Outlet	387.87	385.92	388.17

One of the highest costs in ORC is in the heat transfer units due to their complexity, so it is of high importance to reduce the necessary heat transfer area. R600 obtained the best result with 578.42 m^2, while the heat transfer area for R113 is increased by 10.5% (fig. 10).

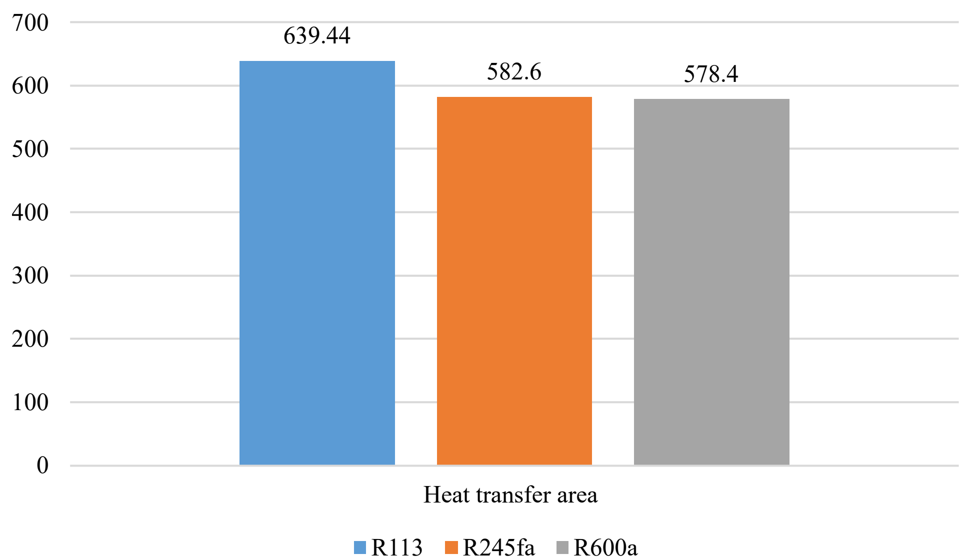

Figure 10: Heat transfer area (HE 1+HE 2) in ORC, (m^2)

Exergy destruction rates for R113, R245fa and R600a presented in percentages are shown in tab. 6. The exergy destruction rate in HE 2 is the highest compared to all the other components, while the one in the pump is the lowest.

Table 6: Exergy destruction rates in ORC for the different fluids

Exergy destruction rates (%)			
	R113	R245fa	R600a
Turbine	8	8	8
Pump	0	3	1
Condenser	0	0	8
HE 1	3	3	3
HE 2	89	86	80

The highest exergy efficiency with 41.64% achieved R113 (fig. 11), which is also in the range reported in the works of other authors.

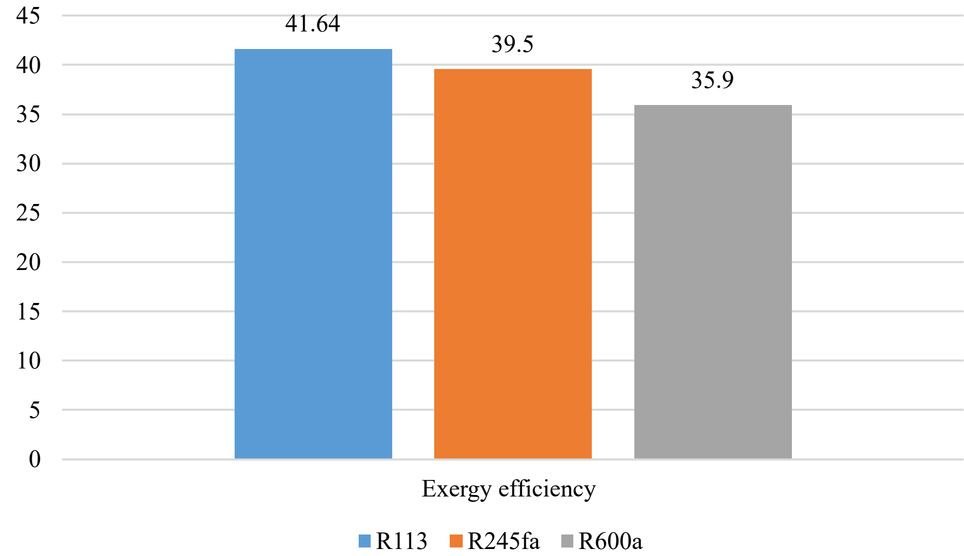

Figure 11: Exergy efficiency of ORC, (%)

If the power plant with previously stated parameters used Serbian lignite as fuel, it would be necessary to provide between 133-169 kt of lignite yearly (fig. 12 a)), which would negatively impact the environment increasing CO_2 emission for about 63-80 kt/year (fig. 12 b)).

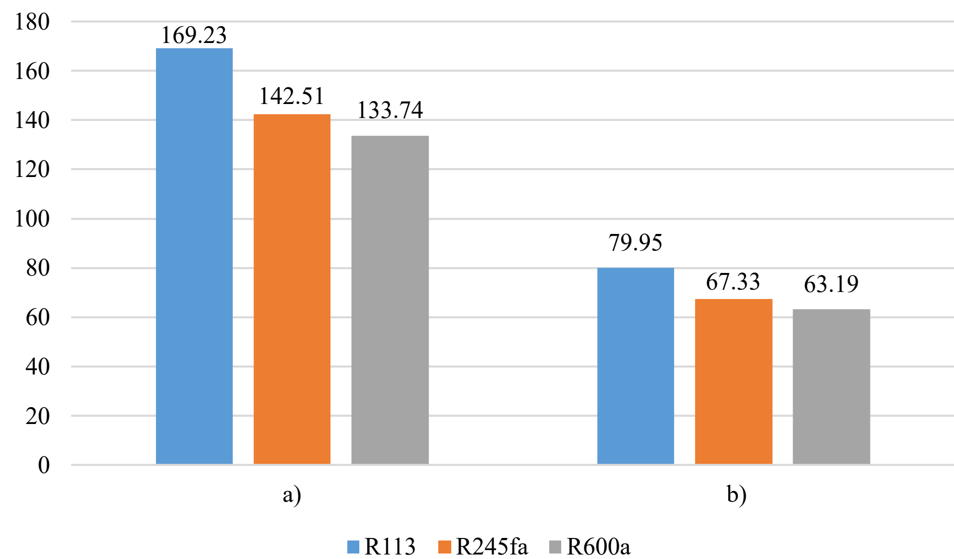

Figure 12: a) lignite consumption per year in ORC, (kt/year), b) equivalent CO_2 emission for the SRC with lignite, (kt/year)

8. Conclusion

In this paper, the simulation and performance study of an ORC with two heat sources was presented. The use of ORC is highly recommended for low-temperature heat sources such as geothermal energy. One of the crucial parts of this research was to use renewable energy sources available in the south of Serbia, especially geothermal energy from Vranjska Banja, which is considered the hottest geothermal spring in Serbia. To improve the efficiency of the process, an additional heat source, wood biomass, was used to achieve a set temperature of working fluid $T_1 = 130°\mathrm{C}$. ORC system consisted of turbine and generator on the same shaft, condenser, pump, and two heat exchangers. The results have been previously discussed, so here are stated most important conclusions:

- R600a obtained the best results regarding mass flow rates of both working and cooling fluid with $51.78\ \mathrm{kg/s}$ and $116.77\ \mathrm{kg/s}$, respectively. Also, it needs the lowest heat transfer area in HE 1 and HE 2.

- R113 provided the highest turbine power output of 4.21 MW for the lowest pump consumption of 73.20 kW , and all followed with the highest thermal and exergy efficiency of 14.53% and 41.64%, respectively.

- The highest exergy destruction rates were noted in HE 2 ($80 - 89\%$), followed by significantly lower destruction rates in the turbine (8%), condenser, and HE $1(3\%)$, while the destruction rates in the pump are meager.

- Scenario 2, which uses lignite as fuel, would need between $133 - 169\ \mathrm{kt}/$ year for the same thermal power input in HE 1 and HE 2 and would contribute to existing $\mathrm{CO_2}$ emission in Serbia for around $63 - 80\ \mathrm{ktCO_2}/$ year.

This study emphasizes the importance of turning to renewable sources, especially geothermal energy, which has the substantial advantage of being independent of weather conditions, and biomass which is considered a carbon-neutral source regarding $\mathrm{CO_2}$ emission. Future research in this area should be obtaining more reliable experimental studies to determine the real performance of the cycle and compare it to the simulation results.

Acknowledgement

This work was financially supported by the Ministry of Education, Science and Technological Development of the Republic of Serbia (Contract No. 451-03-66/2024-03/200105).

Nomenclature

c_p – specific heat capacity at constant pressure, $[\mathrm{kJkg^{-1}K^{-1}}]$
$\dot{E}_x$ – exergy flow rate, [kW]
$\dot{E}_{x\mathrm{D}}$ – exergy destruction rate, [kW]
h – enthalpy, $[\mathrm{kJkg^{-1}}]$
k – coefficient of emission, $[\mathrm{kgkWh^{-1}}]$
LHV – lower heating value, $[\mathrm{kJkg^{-1}}]$
$\dot{m}$ – mass flow rate, $[\mathrm{kgs^{-1}}]$
p – pressure, [Pa]
P – power, [kW]

T – temperature, [K]
$\dot{Q}$ – heat transfer rate, [W]
Greek symbols
η – efficiency, [-]

Subscripts
b – boiler
bm – biomass
c – condensation
e – economiser
ex – exergy
fg – flow gasses
HE – heat exchanger
gw – geothermal water
i – isentropic
P – pump
sat – saturation
sh – superheater
T – turbine
w – water
th – thermal
f – fluid

Abbreviations
GWP – global warm potential
$\mathrm{MD_2M}$ – decamethyltetrasiloxane ORC – Organic Rankine cycle
ODP – ozone depletion potential SRC – Steam Rankine cycle

References

[1] Renewable energy consumption, carbon emissions and human development: Empirical comparison of the trajectories of world regions. In: *Renewable Energy* 179 (2021), pp. 1836–1848. ISSN: 0960-1481.

[2] Merve Senturk. Thermodynamic and economic analysis of geothermal energy powered kalina cycle. In: *Isı Bilimi ve Tekniği Dergisi* 40 (2020), pp. 335–347.

[3] Sylvain Quoilin et al. Techno-economic survey of Organic Rankine Cycle (ORC) systems. In: *Renewable and Sustainable Energy Reviews* 22 (2013), pp. 168–186. ISSN: 1364-0321.

[4] Luca Zanellato et al. Field performance evaluation of geothermal ORC power plants with a focus on radial outflow turbines. In: *Renewable Energy* 147 (2020). ORC in Renewable Energy Systems, ORC 2017 Special Issue, pp. 2896–2904. ISSN: 0960-1481.

[5] Haoshui Yu et al. Optimal design and operation of an Organic Rankine Cycle (ORC) system driven by solar energy with sensible thermal energy storage. In: *Energy Conversion and Management* 244 (2021), pp. 114494. ISSN: 0196-8904.

[6] Yong-qiang Feng et al. Performance prediction and optimization of an organic Rankine cycle (ORC) for waste heat recovery using back propagation neural network. In: *Energy Conversion and Management* 226 (2020), pp. 113552. ISSN: 0196-8904.

[7] Mateusz Świerzewski and Jacek Kalina. Optimisation of biomass-fired cogeneration plants using ORC technology. In: *Renewable Energy* 159 (2020), pp. 195–214. ISSN: 0960-1481.

[8] Jian Song et al. Combined supercritical CO2 (SCO2) cycle and organic Rankine cycle (ORC) system for hybrid solar and geothermal power generation: Thermoeconomic assessment of various configurations. In: *Renewable Energy* 174 (2021), pp. 1020–1035. ISSN: 0960-1481.

[9] Shahram Karimi and Sima Mansouri. A comparative profitability study of geothermal electricity production in developed and developing countries: Exergoeconomic analysis and optimization of different ORC configurations. In: *Renewable Energy* 115 (2018), pp. 600–619. ISSN: 0960-1481.

[10] Ali Bademlioglu et al. A parametric analysis of the performance of organic rankine cycle with heat recovery exchanger and its statistical evaluation. In: *Journal of Thermal Sciences and Technology* 39 (Oct. 2019), pp. 121–135.

[11] Junjiang Bao and Li Zhao. A review of working fluid and expander selections for organic Rankine cycle. In: *Renewable and Sustainable Energy Reviews* 24 (2013), pp. 325–342. ISSN: 1364-0321.

[12] Anil Basaran and Leyla Ozgener. Investigation of the effect of different refrigerants on performances of binary geothermal power plants. In: *Energy Conversion and Management* 76 (2013), pp. 483–498. ISSN: 0196-8904.

[13] Kankeyan Thurairaja et al. Working Fluid Selection and Performance Evaluation of ORC. In: *Energy Procedia* 156 (2019). 5th International Conference on Power and Energy Systems Engineering (CPESE 2018), pp. 244–248. ISSN: 1876-6102.

[14] H.M.D.P. Herath et al. Working fluid selection of Organic Rankine Cycles. In: *Energy Reports* 6 (2020). 2020 The 7th International Conference on Power and Energy Systems Engineering, pp. 680–686. ISSN: 2352-4847.

[15] *Rulebook of energy efficiency, Official Gazette of the Republic of Serbia 61/2011 (2011).*

[16] Stefan Denda Lj et al. Utilization of geothermal springs as a renewable energy source: Vranjska Banja case study. In: *Thermal Science* 23.(6 Part B) (2019), pp. 4083–4093.

[17] Vukašin Šušić, Selim Šaćirović, and Anđelina Marić. Conditions and Possibilities of Geothermal Energy Utilization to Enhance Economic-Touristic Development of Jošanička Banja. In: *Economic Themes* 56.(1) (2018), pp. 91–104.

[18] Dejan Doljak and Tamara Jojic-Glavonjic. State and prospects of geothermal energy usage in Serbia. In: *J. Geogr. Inst. Jovan Cvijic SASA* 66.(2) (2016), pp. 221–236.

[19] Mihailo Milivojevic and Mica Martinovic. Geothermal Energy Possibilities, Exploration and Future Prospects in Serbia. In: *Proceedings World Geothermal Congress* (2005), pp. 24–29.

[20] *Statistical Office of the Republic Serbia. (2024). Statistical Pocketbook of the Republic of Serbia*.

[21] Andjelina Maric and Tomislav Pavlovic. Conditions and possibilities of geothermal energy utilization for economic-touristic development. In: *Journal of the Geographical Institute "Jovan Cvijic", SASA* 68.(2) (2018), pp. 233–248.

[22] Hasan Eren Bekiloğlu, Hasan Bedir, and Günay Anlaş. Multi-objective optimization of ORC parameters and selection of working fluid using preliminary radial inflow turbine design. In: *Energy Conversion and Management* 183 (2019), pp. 833–847. ISSN: 0196-8904.

[23] Kriti Yadav and Anirbid Sircar. Selection of working fluid for low enthalpy heat source Organic Rankine Cycle in Dholera, Gujarat, India. In: *Case Studies in Thermal Engineering* 16 (2019), pp. 100553. ISSN: 2214-157X.

[24] Ljubiša Brkić, Titoslav Živanović, and Dragan Tucaković. *Steam boilers*. 7th. University of Belgrade, Faculty of Mechanical Engineering, 2024. ISBN: 978-86-6060-164-5.

[25] Angelo Algieri and Juraj Šebo. Energetic Investigation of Organic Rankine Cycles (ORCs) for the Exploitation of Low-Temperature Geothermal Sources – A possible application in Slovakia. In: *Procedia Computer Science* 109 (2017). 8th International Conference on Ambient Systems, Networks and Technologies, ANT-2017 and the 7th International Conference on Sustainable Energy Information Technology, SEIT 2017, 16-19 May 2017, Madeira, Portugal, pp. 833–840. ISSN: 1877-0509.

[26] Christopher Koroneos et al. Exergy analysis for a proposed binary geothermal power plant in Nisyros Island, Greece. In: *Geothermics* 70 (2017), pp. 38–46. ISSN: 0375-6505.

[27] Carlos Eymel Campos Rodríguez et al. Exergetic and economic comparison of ORC and Kalina cycle for low temperature enhanced geothermal system in Brazil. In: *Applied Thermal Engineering* 52.(1) (2013), pp. 109–119. ISSN: 1359-4311.

[28] Hadi Ganjehsarabi, Ali Gungor, and Ibrahim Dincer. Exergetic performance analysis of Dora II geothermal power plant in Turkey. In: *Energy* 46.(1) (2012). Energy and Exergy Modelling of Advance Energy Systems, pp. 101–108. ISSN: 0360-5442.

[29] Mehmet Kanoglu and Ali Bolatturk. Performance and parametric investigation of a binary geothermal power plant by exergy. In: *Renewable Energy* 33.(11) (2008), pp. 2366–2374. ISSN: 0960-1481.

[30] A.F. Altun and M. Kilic. Thermodynamic performance evaluation of a geothermal ORC power plant. In: *Renewable Energy* 148 (2020), pp. 261–274. ISSN: 0960-1481.

[31] Ljubiša Brkić, Titoslav Živanović, and Dragan Tucaković. *Thermal calculation of steam boilers*. 6th. University of Belgrade, Faculty of Mechanical Engineering, 2022. ISBN: 978-86-6060-129-4.

Submitted: 08.02.2025
Revised: 31.03.2025
Accepted: 04.04.2025